Effects of chitooligosaccharide-zinc on mice ovarian function in premature ovarian failure via regulating the sestrin2/nrf2 signaling pathway

Jia Li (490780258@qq.com)
Nanchang University
Yuhang Chen
Nanchang University
Jiayu Xu
Nanchang University
Jiangying Liu
Nanchang University
Jiacheng Fu
Nanchang University
Xiuping Cao
Nanchang University
Jian Huang
Nanchang University
Yuehui Zheng
Nanchang University

Research

Keywords: Premature ovarian failure, Chitooligosaccharide-zinc, sestrin2-nrf2, ovarian function, aging

Posted Date: January 2nd, 2020

DOI: https://doi.org/10.21203/rs.2.19856/v1

Abstract

Background

The chitosan oligosaccharide-zinc (COS·Zn) is also a powerful antioxidant and anti-aging scavenger, whose anti-oxidative ability immensely exceeds that of vitamin C. Therefore, this study aimed to investigate the protective effects and potential mechanism by which COS·Zn improves ovarian function and delays aging in POF.

Methods

The female KM adult mice and POF mice were divided into treated and prevention groups; these were prophylactically or therapeutically administered COS·Zn (150mg/kg·d, 300mg/kg·d) for 21 days, respectively.

Results

The number of antral follicles in COS·Zn-treated groups was lower in the treated and prevention groups than that in the control group, respectively. Obviously, the ovarian index, the level of FSH and LH all increased notably during the 300 mg/kg·d treated group and the prevention group compared with cy/bus groups. The expression of MVH, OCT4 and PCNA in the 300 mg/kg·d treated groups and MVH in the prevention groups were remarkably increased compared with the CY/BUS group. Meanwhile, the protein levels of P53 and P16 were markedly down-regulated in the treated groups and prevention groups compared with CY/BUS, except for the expression of P53 in the prevention groups. Furthermore, the Sestrin2 (SESN2) and SOD2 proteins were significantly higher in the 150 mg/kg·d treated group compared with the CY/BUS group, but the 300 mg/kg·d and CY/BUS group showed no significant difference in the level of SESN2. Similarly, the NRF2 and SESN2 proteins were up-regulated in the prevention groups, and the change in SOD2 was not significant. The results revealed increased GSH levels in the 150 mg/kg·d and 300 mg/kg·d treated groups compared with CY/BUS group, and the same trend was also shown in the prevention groups.[1]

Conclusion

COS·Zn improves ovarian and follicular developmental defects caused by regulating the sestrin2-nrf2 signaling pathway, and these results suggest a novel product that is effective a POF prevention and treatment drug.

1. Introduction

Premature ovarian failure (POF), as the main cause of ovogenic infertility, refers to the development of amenorrhea due to the cessation of ovarian function before the age of 40 years [1-3]. A wide spectrum of pathogenic mechanisms may lead to the development of POF, including chromosomal, genetic, autoimmune, metabolic (galactosemia), infectious (mumps) and iatrogenic (anticancer treatments)

causes [4-6]. In the degenerative process, mitochondrial dysfunction causes the overproduction of reactive oxygen species (ROS), which results in oxidative damage. Oxidative stress may play a role in the degeneration process of POF, which could be more pronounced in the POF population and could impair antioxidant defenses and increase susceptibility to oxidative stress and damage [1, 7, 8]. Therefore, oxidative damage is considered inevitable in POF, and the theory of oxidative-stress-related ovarian damage has attracted increasing attention.

Nowadays, no effective therapies for POF are available. Chitosan oligosaccharide (COS) molecules contain a large number of active amino and hydroxyl groups [9], and can be chelated with inorganic zinc to produce an organic form of chitooligosaccharide-zinc (COS·Zn) by controlling the reaction conditions [10, 11]. As a basic amino oligosaccharide, COS·Zn is also a powerful antioxidant and anti-aging scavenger [12], whose anti-oxidative ability immensely exceeds that of vitamin C. Cumulative evidence suggests that COS·Zn possesses biological properties against oxidative stress in different organs and tissues [13-15]. One study has reported that COS·Zn effectively reduced the content of MDA in D-galactose-treated mice and significantly increased the activities of SOD, T-AOC, GSH-Px and CAT in the serum, kidney and liver of the mouse model; in particular, the effect of protective enzymes in serum is better than in the COS, $ZnSO_4$ and COS+$ZnSO_4$ mixture groups [13].

Moreover, some studies have reported that COS·Zn is associated with regulation of the growth and development of the reproductive system in mice, and plays a major role in improvement of the tissue structure of reproductive organs/fertility in female and male mice. Another study has indicated that the relationship between COS·Zn and mammalian ovarian function is closely related [16]. The COS·Zn-treated group could obviously improve the female fertility rate, resulting in an increased number of ovarian follicles and endometrial thickness, an abundance in the uterine glands, increased egg vitality and fertilization [8]. However, in the process of POF, the oxidative damage to ovaries could not be avoided, so we included COS·Zn in our histological study to determine the effect of oxidative damage on POF, in consideration of the potential of COS·Zn in therapies for POF.

In mammals, the Sestrin family comprises three members (Sestrin 1-3), which can be induced by oxidative stress and DNA damage in a p53-dependent manner [17-20]. Sestrin2 (Sesn2), a highly conserved protein, is an essential member of the Sestrin family, which is also expressed in endothelial and macrophage cells, where it displays a protective role [21, 22]. Our research has also shown that Sestrin is strongly expressed in ovarian tissue; however, the exact mechanism for ovarian-protective effects have not been clearly elucidated. To date, the cellular function of Sestrin2 (SESN2) has been well recognized; however, the effect on ovarian function has not been fully determined.

As an important endogenous antioxidant factor, NF-E2-related factor 2 (NRF2) is an essential part of the oxidative stress response [23-25]. In oxidative stress injury, NRF2 is separated from Keap1 (Kelch-like ECH-associated protein 1) and enters the nucleus [26-29]. When combined with antioxidant response elements (AREs), the expression of phase II detoxification enzymes and antioxidants is regulated by multiple signaling pathways, such as sulfiredoxin1 (Srx1) and thioredoxin1 (Trx1) [30]. Studies have

indicated that NRF2 is mainly regulated by Keap1 [31], and that NRF2 plays an important role in regulating ovarian dysfunction and treating ovarian cancer [32-35]. Further studies have clarify that SESN2 could both directly and indirectly participate in the regulation of NRF2 in the process of metabolism [19, 36]. However, despite NRF2 being shown to be involved in many signaling pathways, the specific mechanism and functional effects are not completely understood.

The protective effects of COS·Zn against oxidative damage have not been clarified in POF, and there are no similar studies available. Therefore, this study was undertaken to demonstrate the protection against oxidative damage in POF to determine whether COS·Zn would, in part, ameliorate ovarian function. If COS·Zn shows protective effects in POF, dietary COS·Zn could serve as a medicine against oxidative damage.

2. Material And Methods

2.1 Ethical approval

All procedures with animals were approved by the Institutional Animal Care and Use Committee of Nanchang, and were performed in accordance with the National Research Council Guide for the Care and Use of Laboratory Animals.

2.2 The preparation of COS·Zn

COS·Zn was prepared under optimal reaction conditions, which were determined in the study of Jin Yue [11]. COS and zinc sulfate were weighed with a mass ratio of 2:1 and respectively dissolved in two beakers with equal amounts of distilled water. Then the two solutions were mixed in equal volumes and the pH was slowly adjusted to 7 with 1% ammonium hydroxide solution. The mixture was then chelated at 40°C for about 30 minutes, and anhydrous ethanol at three times the volume of the mixture was slowly added to it. After rinsing with anhydrous ethanol, the product was dried in a 60°C oven for several hours to obtain a yellow powder, which was just COS·Zn. The zinc content of the COS·Zn prepared with this method was 10%.

2.3 Mice and treatments

Female KM mice aged 6 weeks (weighed 20-25g), purchased from the Laboratory Animal Center of Nanchang University, were allowed to adapt to the facility for at least 7 days before the experiment started. Food and water were abundant at all times. The temperature was maintained at 22±1°C. Each mouse received a 12h cycle of brightness and darkness, and mice were randomly divided into the treatment and prevention groups, with 6 mice in each.

Each group of mice, except the control group and COS·Zn+CY/BUS group, was administered CY/BUS for 21 days to build the models of premature ovarian failure (POF). The mice in the COS·Zn+CY/BUS group were prophylactically administered COS·Zn (300mg/kg.d) for 21 days. No special operations were offered to the control group.

The mass ratio of COS to Zn in the COS·Zn synthesized in our laboratory is 9:1, and all of the concentrations of COS·Zn mentioned in this article were measured by COS (Fig. 1). Based on the literature review and our actual observation results, it was determined that the daily food intake of the experimental mice was about 6g, which means that every mouse in the COS·Zn (150mg/kg.d) group requires 1mg COS·Zn per day and 2mg COS·Zn per day in the COS·Zn (300mg/kg.d) group. We took 0.04g COS·Zn powder, dissolved in 8mL normal saline, shaken and mixed, and added 2mL sodium carboxymethyl cellulose to prevent the deposition of COS·Zn powder; this was shaken and mixed again, to make a 4mg/mL COS·Zn solution. After the establishment of POF models, the mice underwent the following procedures: (1) the COS·Zn (150mg/kg.d) group was administered 0.125mg/mL COS·Zn solution per day by intragastric (IG) administration for 21 days; (2) the COS·Zn (300mg/kg.d) group was administered 0.25mg/mL COS·Zn solution per day by IG administration for 21 days; (3) the COS·Zn+CY/BUS group received CY/BUS by intraperitoneal (IP) injection; and (4) the control and CY/BUS groups received 0.25mL normal saline per day by IG administration for 21 days.

2.4 Histological analysis of ovarian tissue and ovarian follicle count

Mice were killed by cervical dislocation. The ovaries were collected, and fixed in 4% paraformaldehyde, before they were embedded in paraffin, as described previously [37]. The paraffin-embedded ovaries were cut into serial sections and stained using hematoxylin and eosin (HE). The ovarian follicles were counted as described previously [38,39]. Immunostaining of the ovaries from mice from the treated and prevention groups was performed according to previously published procedures [40].

The primary antibodies used in this study were as follows: anti-MVH (1:100, ab27591), anti-OCT4 (1:100, ab18976), anti-PCNA (1:100, ab56701), anti-P53 (1:100, ab54073), anti-P16 (1:100, ab54073), anti-IL2 (1:100, ab54073), anti-IL4, anti-TNF-α, anti- NRF2, anti-Sestrin2 and anti-SOD2 (1:100, ab51134). The secondary antibodies used in this study were goat anti-mouse and goat anti-rabbit IgG conjugated with fluorescein isothiocyanate at a dilution of 1:200 (proteintech, China). All of the images were taken using a NIKON Eclipse 80i microscope.

2.5 Western blotting

Total protein was extracted from different ovarian tissues with RIPA lysis solution (Beyotime, P0013C). The proteins were subjected to SDS-PAGE (sodium dodecyl sulfate-polyacrylamide gel electrophoresis) and then transferred to PVDF membranes (Millipore Corp., Bedford, MA) before being processed according to the antibody manufacturer's instructions. The antibodies used for western blotting were anti-MVH (1:100, ab27591), anti-OCT4 (1:100, ab18976), anti-PCNA (1:100, ab56701), anti-P53 (1:100, ab54073), anti-P16 (1:100, ab54073), anti-NRF2, anti-Sestrin2 and anti-SOD2 (1:100, ab51134). The results were analyzed by the gel imaging and analysis system and converted to semi-quantitative data by the Gelscan software. The level of β-actin was quantified at the same time as an internal quantitative control. Each experiment was repeated at least three times.

2.6 Tunnel assay

The apoptotic rates of ovarian sections were detected by terminal deoxynucleotidyl transferase mediated dUTP-biotin nick end labeling (TUNEL), and the procedure was performed using an Apoptosis Detection Kit (Solarbio Biotech Co., Ltd., Beijing, China) according to the manufacturer's instructions. After being treated with TUNEL reaction mixture for 1 h, the sections were washed twice with PBS for 10 min and counterstained with 4',6-diamidino-2-phenylindole (DAPI) (Sigma-Aldrich) for 5 min. Washing was then performed three times with ddH_2O. A confocal laser scanning microscope (Leica, TSP8) was used to photograph sections, and the apoptotic rate was analyzed using IPP 6.0 Software.

2.7 SOD and GSH detection

Superoxide dismutase (SOD): SOD was assessed using the WST-1 method. Blank wells, standard wells, determination wells and control wells were prepared according to the experimental requirements. Serum from mice was incubated at 37°C for 20 min. The absorbance value of each well at 450 nm was detected by a microplate reader.

Malondialdehyde (GSH): GSH was determined using the thiobarbituric acid method. According to the instructions provided by Shanghai GeneChem Biotechnology Co., Ltd. (Shanghai, China), blank wells, standard wells, determination wells and control wells were prepared. The absorbance value of each well at 450 nm was detected by a microplate reader (1 cm of optical path, set zero by distilled water).

2.8 Hormone level measurement

Blood was drawn from the orbital socket and serum was collected. The levels of E2 and FSH were measured by the biological company.

2.9 Statistical methods

All analyses were performed using GraphPad Prism 5.0 (GraphPad Software, Inc., San Diego, CA). The statistical comparisons between different groups were analyzed by Student's paired *t*-test. The threshold of $p < 0.05$ was considered significant; $p < 0.01$ and $p < 0.001$ were each considered extremely significant.

3. Results

3.1 The preparation of COS·Zn by infrared spectroscopic analysis

The bimodal C=O bond disappeared at about 1600 cm^{-1}, and the absorption peak obviously weakened; these data indicate that the C-O double bond chelates with the zinc ion in the COS molecule and forms "C.O-Zn". The results of infrared spectroscopy showed that COS chelates with the zinc ion and forms a stable chelate which is known as "COS·Zn" (Fig. 1a, b).

3.2 COS·Zn supplementation improves ovarian and follicular developmental defects caused by POF in mice

Ovarian morphology of the control and treatment groups (150, 300mg/kg·d COS·Zn-treated groups) was determined by HE staining (Fig. 2a). The numbers of primary follicles, secondary follicles, corpus, and atretic follicles were counted (Fig. 2a). In the 150 mg/kg·d group, we found that the number of antral follicles in the COS·Zn-treated groups was lower than that in the control group ($p < 0.05$), and their numbers were dramatically reduced in CY/BUS groups and the 300 mg/kg·d group ($p < 0.05$), but the 150 mg/kg·d and 300 mg/kg·d COS·Zn-treated groups were not significantly different. The numbers of primary follicles and secondary follicles were significantly higher in the 150 mg/kg·d and 300 mg/kg·d COS·Zn-treated groups compared with the control group ($p < 0.01$, $p < 0.05$). However, the number of primary follicles was significantly higher in the 300 mg/kg·d COS·Zn-treated group compared with the CY/BUS group ($p < 0.05$). Obviously, we found that the ovarian index (ovarian weight/body weight ratio), and levels of FSH and LH all increased notably in the 300 mg/kg·d COS·Zn-treated and CY/BUS groups ($p < 0.05$, $p < 0.001$, (Fig. 2b, c).

To further clarify the changes in the amounts of follicles and their proportion between different treated groups, we analyzed the prevention groups (300mg/kg.d COS·Zn-treated group) using HE staining. The results showed a decrease in antral follicles in the prevention group compared to the control group (Fig. 3a, $p < 0.01$). We also found that the numbers of primary and secondary follicles increased in the prevention group and control group; however, for the prevention-ovary index, the level of FSH and LH were all dramatically increased in the prevention group compared with the control and CY/BUS groups, respectively (Figs. 3b, c, $p < 0.01$, $p < 0.001$). Collectively, the data suggest that COS·Zn (300mg/kg.d) improves the level of ovarian and follicle damage by POF.

3.2 COS·Zn supplementation improved ovarian function in the POF in mice

To evaluate changes in the ovarian functions of COS·Zn-treated mice, we first detected the expression of MVH and OCT4. The results revealed increased MVH and OCT4 levels in the 300 mg/kg·d COS·Zn-treated groups compared with the CY/BUS group (Fig.4a, c, $p< 0.05$, $p < 0.001$). The changes in MVH were observed with a significant increase in the COS·Zn-prevention groups (Fig.4b, e, $p < 0.01$). In addition, PCNA levels also increased during the 150 mg/kg.d.d and 300 mg/kg.d.d COS·Zn-treated groups compared with the CY/BUS group (Fig.4a,c, $p < 0.05$); this trend was also detected in the control and COS·Zn-prevention groups (Fig.4b,e, $p < 0.05$). Using the Tunnel assay, we found that the apoptotic signal was negative in granulosa cells and oocytes (Fig.4d, f). The number of apoptotic cells per section in the 300 mg/kg.d.d COS·Zn-treated groups was significantly lower than that in the control and CY/BUS groups.

Meanwhile, the protein levels of P53 and P16 were markedly down-regulated in the treated and prevention groups compared with CY/BUS, except for the expression of P53 in the prevention groups (Fig.5a, b).

3.3 COS·Zn causes oxidative stress status and anti-aging capacity to increase by regulating the sestrin2-nrf2 signaling pathway in the POF mice

To investigate causes of the changes in ovarian function, we detected the oxidative stress status and anti-aging capacity in ovaries using COS·Zn-treated mice. In the treated groups, the protein level of NRF2 in the 150 mg/kg.d.d and 300 mg/kg.d.d COS·Zn-treated groups were markedly increase (Fig.6a, $p < 0.05$). Meanwhile, the SESN2 and SOD2 proteins were significantly higher in the 150 mg/kg.d.d compared with the CY/BUS groups (Fig.6a, $p < 0.01$, $p < 0.001$), but the 300 mg/kg.d.d and CY/BUS groups showed no significant difference in the level of SESN2. Similarly, the NRF2 and SESN2 proteins were up-regulated in the COS·Zn-prevention groups (Fig.6c,$p < 0.05$), and the change in SOD2 exhibited no significant effect. We then analyzed changes in the GSH and SOD2 levels in different groups. The results revealed increased GSH and SOD2 levels in the 150 mg/kg.d.d and 300 mg/kg.d.d COS·Zn-treated groups compared with the CY/BUS group (Fig.6b), and the same trend was shown in the COS·Zn-prevention groups (Fig.6d).

4. Discussion

COS·Zn showed good anti-aging effects and enhanced immune function in previous studies, as documented by Hao et al. [13], who found that the scavenging effect of COS·Zn complexes was significantly better than that of COS, $ZnSO_4$ and COS+$ZnSO_4$ [13]. At the same time, with an increase in the concentrations of COS·Zn, the scavenging ability of DPPH free radicals gradually increased [41]. According to the references, the successful synthesis of COS·Zn was investigated by infrared spectroscopic analysis which showed that COS chelates with zinc ions and forms a stable chelate [41]. However, there are several studies devoted to the roles of COS·Zn, including the inhibitory activity of microorganisms, and improved organ index for the liver, thymus, spleen, and kidney. Notably, the ovary was the major target organ, so the aim of the present study was to analyze the anti-oxidative effect of COS·Zn on the ovarian function of POF mice.

In treated groups, our study showed that the numbers of primary and secondary follicles were significantly increased in the 300mg/kg·d COS·Zn-treated group, and atretic follicles were also decreased in the 300mg/kg·d COS·Zn groups. Furthermore, the ovarian index results further suggested that COS·Zn decelerated apoptosis in ovaries and advanced ovarian follicular development, which is consistent with previous studies [16]. Collectively, the data suggest that COS·Zn (300mg/kg·d) improved the level of ovarian and follicle damage in POF. Thus, the preparation groups were treated with 300mg/kg·d COS·Zn. The decrease in antral follicles in the prevention groups was like that in the treatment groups. We also found that the numbers of primary and secondary follicles increased in the prevention groups. Meanwhile, regarding the prevention-ovary index, the levels of FSH and LH were all dramatically increased in the prevention groups compared with the control and CY/BUS groups, respectively. Therefore, the development of the ovary was promoted by COS·Zn treatment in POF mice. Follicular development-related genes may play certain roles in this process [42]. Surprisingly, the changes in MVH, PCNA and OCT4 observed a significant increase in the COS·Zn groups compared with normal and CY/BUS mice.

To further examine the mechanism of COS·Zn on the ovaries, we performed ovarian proteomic analysis. Sestrin2/NRF2 is probably the most important master of the expression of molecules that exert antioxidant functions within organs and cells. In the ovaries of POF mice, COS·Zn up-regulates the levels of Sestrin2, NRF2 and SOD2, which are responsible for the antioxidant effects. Taken together, COS·Zn improves ovarian and follicular developmental defects caused by regulating the sestrin2-nrf2 signaling pathway, and these results suggest a novel product that is effective a POF prevention and treatment drug.

5. Conclusion

In reproduction, no effective therapies for POF are available. COS·Zn is the basic and primary requirement for the growth and development of the reproductive system in mice[16], and plays a major role in improvement of the tissue structure of reproductive organs/fertility in female and male mice. Increasing the level of COS·Zn is an effective way to improve ovarian and follicular development caused by regulating the sestrin2-nrf2 signaling pathway, and these results suggest a novel product that is effective a POF prevention and treatment drug.

6. Abbreviations

POF: Premature ovarian failure; COS·Zn: Chitooligosaccharide-zinc; HE: Hematoxylin Eosin; MVH: Mouse vasa homologue; PCNA: Proliferating cell nuclear antigen; OCT4: Octamer binding transcription factor 4; CY/BUS: Cyclophosphamide/Busulfan; GSH: Glutathione; SOD2: superoxide dismutase2; E2: Estradiol; FSH: ,follicle stimulating hormone.

7. Declarations

Acknowledgements

Not applicable.

Authors' contributions

Jia Li: Conception and design of study, drafting the manuscript. Yuhang Chen: Analysis and / or interpretation of data. Jiaye Xu: Analysis and / or interpretation of data. Jiangying Liu: Analysis and / or interpretation of data. Jiachen Fu and Xiuping Cao: Acquisition of data. Jian Huang: modify the manuscript. Yuehui Zheng: Conception and design of study, acquisition of data, revising the manuscript critically for important intellectual content. All authors read and approved the final manuscript.

Funding

This work was supported by the Natural Science Foundation of Jiangxi, China (grant numbers: 2018ACB20018, 20192BAB215009), the National Natural Science Foundation of China (grant number:

31460307,81671455,81771583) and the young teachers research and training foundation of Nanchang university medical department (grant number: PY201814).

Availability of data and materials

The datasets used and/or analysed during the current study are available from the corresponding author on reasonable request.

Ethics approval and consent to participate

Our study protocol was approved by the Institutional Animal Care and Use Committee of Nanchang, and were performed in accordance with the National Research Council Guide for the Care and Use of Laboratory Animals.

Consent for publication

Not applicable.

Competing interests

The authors declare that they have no competing interests

8. References

1. Dada, R., et al., Chromosomal abnormalities & oxidative stress in women with premature ovarian failure (POF). The Indian Journal of Medical Research, 2012. 135(1): p. 92-97.
2. Alkhammash, S., J. Saumet, and G. Genest, Infertility and pregnancy in patients with autoimmune polyendocrinopathy-candidiasis-ectodermal dystrophy: More than just primary ovarian failure? Am J Reprod Immunol, 2019. 82(4): p. e13169.
3. Zhang, P., et al., Clinical analysis of Chinese infertility women with premature ovarian failure. Neuro Endocrinol Lett, 2007. 28(5): p. 580-4.
4. Delkhosh, A., et al., Upregulation of FSHR and PCNA by administration of coenzyme Q10 on cyclophosphamide-induced premature ovarian failure in a mouse model. J Biochem Mol Toxicol, 2019: p. e22398.
5. Herraiz, S., et al., Treatment potential of bone marrow-derived stem cells in women with diminished ovarian reserves and premature ovarian failure. Curr Opin Obstet Gynecol, 2019. 31(3): p. 156-162.
6. Lee, D.H., et al., Identification of serum biomarkers for premature ovarian failure. Biochim Biophys Acta Proteins Proteom, 2019. 1867(3): p. 219-226.
7. Verma, P., et al., Role of Trace Elements, Oxidative Stress and Immune System: a Triad in Premature Ovarian Failure. Biol Trace Elem Res, 2018. 184(2): p. 325-333.
8. Lim, J., et al., Glutamate Cysteine Ligase Modifier Subunit (Gclm) Null Mice Have Increased Ovarian Oxidative Stress and Accelerated Age-Related Ovarian Failure. Endocrinology, 2015. 156(9): p. 3329-

43.
9. Wang, X.Y., et al., Molecular dynamics of paclitaxel encapsulated by salicylic acid-grafted chitosan oligosaccharide aggregates. Biomaterials, 2013. 34(7): p. 1843-51.
10. Ying, J., et al., Coordination Characteristics of Chitosan on Zn/Fe Ions and the Application of the Coordination Compound. Modern Food Science and Technology, 2007. 23(9): p. 88-92.
11. Yue, J., Preparation of zinc-COS and comparative study of its nutritional functions. 2011, Liaoning Normal University.
12. Jia, Z., et al., Antioxidant Activities of Chitooligosaccharide and Its Derivaties. Progress in Veterinary Medicine, 2015. 36(7): p. 118-121.
13. Guijuan, H., et al., Antioxidant Effect of Chitooligosaccharide-zinc Complex on the Oxidative Aging Mice Model. Journal of Nuclear Agricultural Sciences, 2019. 33(6): p. 1156-1164.
14. Xiao-lin, T., Effect of Chitooligosaccharide-Zinc on Growth and Reproduction Performance of Kunming Mice. 2013, Liaoning Normal University.
15. Hua, Z., et al., Research Progress on Regulatory Effect and Mechanism of Chitooligosaccharides on Immunity and Inflammation in Animals. Chinese Journal of Animal Nutrition, 2019. 31(1): p. 15-23.
16. Xiao-lin, T., et al., Effect of Chitooligosaccharide-Zinc on Growth and Reproduction Performance in Female Kunming Mice. ACTA Nutrimenta SINICA, 2013. 35(3): p. 262-267.
17. Deng, W., et al., p53 coordinates decidual sestrin 2/AMPK/mTORC1 signaling to govern parturition timing. J Clin Invest, 2016. 126(8): p. 2941-54.
18. Liu, S.Y., Y.J. Lee, and T.C. Lee, Association of platelet-derived growth factor receptor beta accumulation with increased oxidative stress and cellular injury in sestrin 2 silenced human glioblastoma cells. FEBS Lett, 2011. 585(12): p. 1853-8.
19. Tomasovic, A., et al., Sestrin 2 protein regulates platelet-derived growth factor receptor beta (Pdgfrbeta) expression by modulating proteasomal and Nrf2 transcription factor functions. J Biol Chem, 2015. 290(15): p. 9738-52.
20. Wang, J.M., et al., Sestrin 2 protects against metabolic stress in a p53-independent manner. Biochem Biophys Res Commun, 2019. 513(4): p. 852-856.
21. Kim, M.J., et al., SESN2/sestrin2 suppresses sepsis by inducing mitophagy and inhibiting NLRP3 activation in macrophages. Autophagy, 2016. 12(8): p. 1272-91.
22. Dai, J., et al., [Sestrin 2(SESN2) promotes primary resistance to sorafenib by activating AKT in hepatocellular carcinoma cells]. Xi Bao Yu Fen Zi Mian Yi Xue Za Zhi, 2018. 34(5): p. 427-433.
23. Farruggia, C., et al., Astaxanthin exerts anti-inflammatory and antioxidant effects in macrophages in NRF2-dependent and independent manners. J Nutr Biochem, 2018. 62: p. 202-209.
24. Jiang, P., et al., Chotosan ameliorates cognitive impairment and hippocampus neuronal loss in experimental vascular dementia via activating the Nrf2-mediated antioxidant pathway. J Pharmacol Sci, 2019. 139(2): p. 105-111.

25. Radan, M., et al., In vivo and in vitro evidence for the involvement of Nrf2-antioxidant response element signaling pathway in the inflammation and oxidative stress induced by particulate matter (PM10): the effective role of gallic acid. Free Radic Res, 2019. 53(2): p. 210-225.
26. Li, X.N., et al., Resveratrol protects against oxidative stress by activating the Keap-1/Nrf2 antioxidant defense system in obese-asthmatic rats. Exp Ther Med, 2018. 16(6): p. 4339-4348.
27. Paunkov, A., et al., A Bibliometric Review of the Keap1/Nrf2 Pathway and its Related Antioxidant Compounds. Antioxidants (Basel), 2019. 8(9).
28. He, X., et al., Protection against chromium (VI)-induced oxidative stress and apoptosis by Nrf2. Recruiting Nrf2 into the nucleus and disrupting the nuclear Nrf2/Keap1 association. Toxicol Sci, 2007. 98(1): p. 298-309.
29. Sharath Babu, G.R., et al., Pelargonidin Modulates Keap1/Nrf2 Pathway Gene Expression and Ameliorates Citrinin-Induced Oxidative Stress in HepG2 Cells. Front Pharmacol, 2017. 8: p. 868.
30. Zhang, L.L. and Z.J. Zhang, Sestrin2 aggravates oxidative stress of neurons by decreasing the expression of Nrf2. Eur Rev Med Pharmacol Sci, 2018. 22(11): p. 3493-3501.
31. Mishra, M., Q. Zhong, and R.A. Kowluru, Epigenetic modifications of Keap1 regulate its interaction with the protective factor Nrf2 in the development of diabetic retinopathy. Invest Ophthalmol Vis Sci, 2014. 55(11): p. 7256-65.
32. Cho, H.Y., et al., Expression Patterns of Nrf2 and Keap1 in Ovarian Cancer Cells and their Prognostic Role in Disease Recurrence and Patient Survival. Int J Gynecol Cancer, 2017. 27(3): p. 412-419.
33. Czogalla, B., et al., Correlation of NRF2 and progesterone receptor and its effects on ovarian cancer biology. Cancer Manag Res, 2019. 11: p. 7673-7684.
34. Konstantinopoulos, P.A., et al., Keap1 mutations and Nrf2 pathway activation in epithelial ovarian cancer. Cancer Res, 2011. 71(15): p. 5081-9.
35. Wu, X., et al., The Study of Nrf2 Signaling Pathway in Ovarian Cancer. Crit Rev Eukaryot Gene Expr, 2018. 28(4): p. 329-336.
36. Shin, B.Y., et al., Nrf2-ARE pathway regulates induction of Sestrin-2 expression. Free Radic Biol Med, 2012. 53(4): p. 834-41.
37. Yang Y, Lin P, Chen F, Wang A, Lan X, Song Y, Jin Y. Luman recruiting factor regulates endoplasmic reticulum stress in mouse ovarian granulosa cell apoptosis. Theriogenology. 2013.79(4): p. 633-9.
38. Tilly JL. Ovarian follicle counts--not as simple as 1, 2, 3. Reprod Biol Endocrinol. 2003.1: p.11.
39. Takai, Y., et al., Bax, caspase-2, and caspase-3 are required for ovarian follicle loss caused by 4-vinylcyclohexene diepoxide exposure of female mice in vivo. Endocrinology, 2003. 144(1): p. 69-74.
40. Wenqi, L., et al., The Changes of C-kit in Premature Ovarian Failure in Ovary of Rats. Anatomy Research, 2017. 39(2): p. 85-87,92.
41. Xu-hong, Y., et al., DPPH Scavenging Activity of Chitosan oligosaccharide Zinc Complexes. Journal of Food Science and Biotechnology 2009. 28(3): p. 329-331.

42. Li, Y., et al., Prepubertal bisphenol A exposure interferes with ovarian follicle development and its relevant gene expression. Reproductive toxicology, 2014. 44: p. 33-40.

Figures

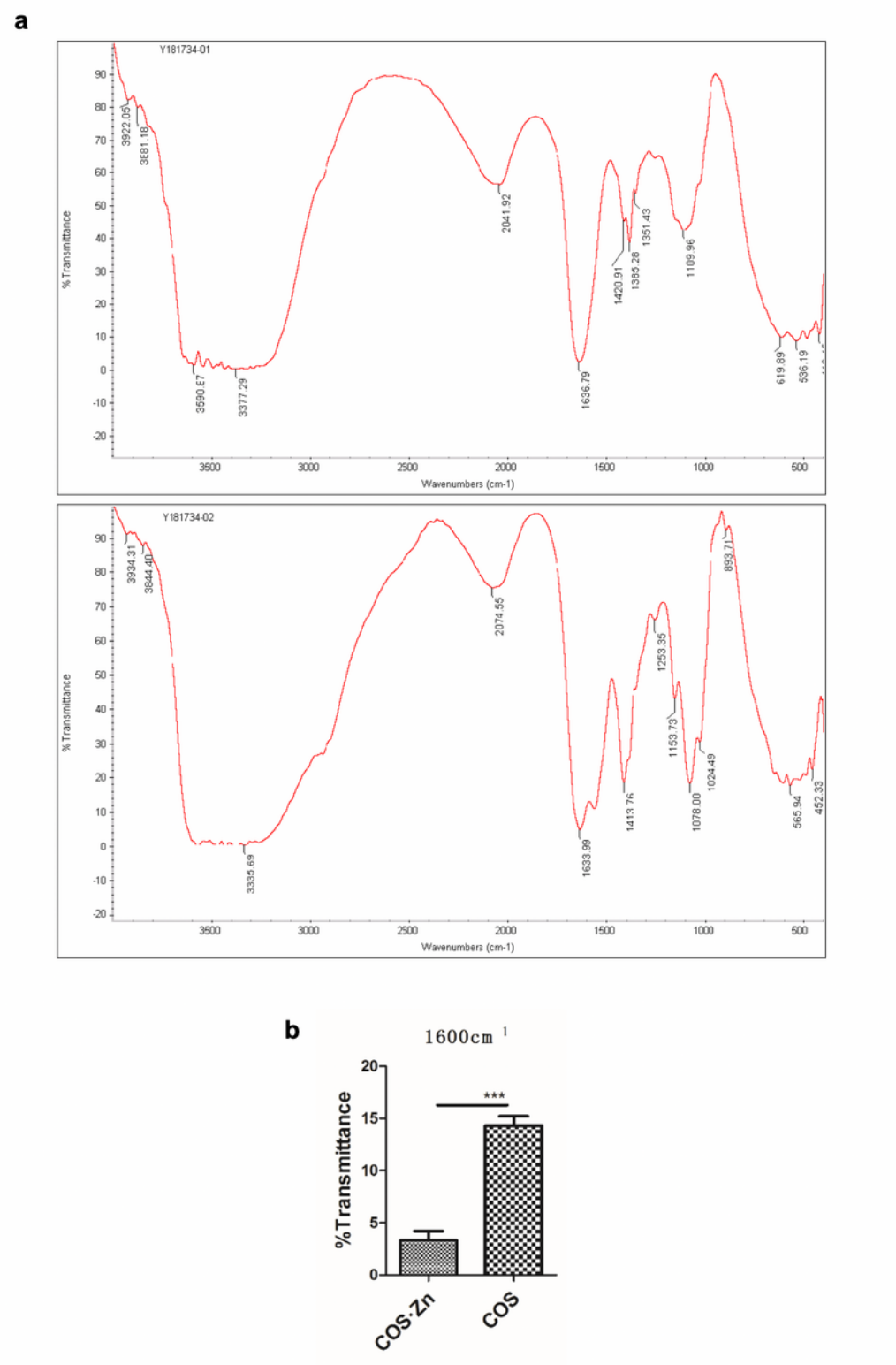

Figure 1

The result of COS•Zn by the infrared spectroscopic analysis. (a) The preparation of COS·Zn and COS. (b) The analysis of transmittance during the COS·Zn and COS. The wavenumber is 1600cm-1. *p<0.05, **p<0.01, ***p<0.001.

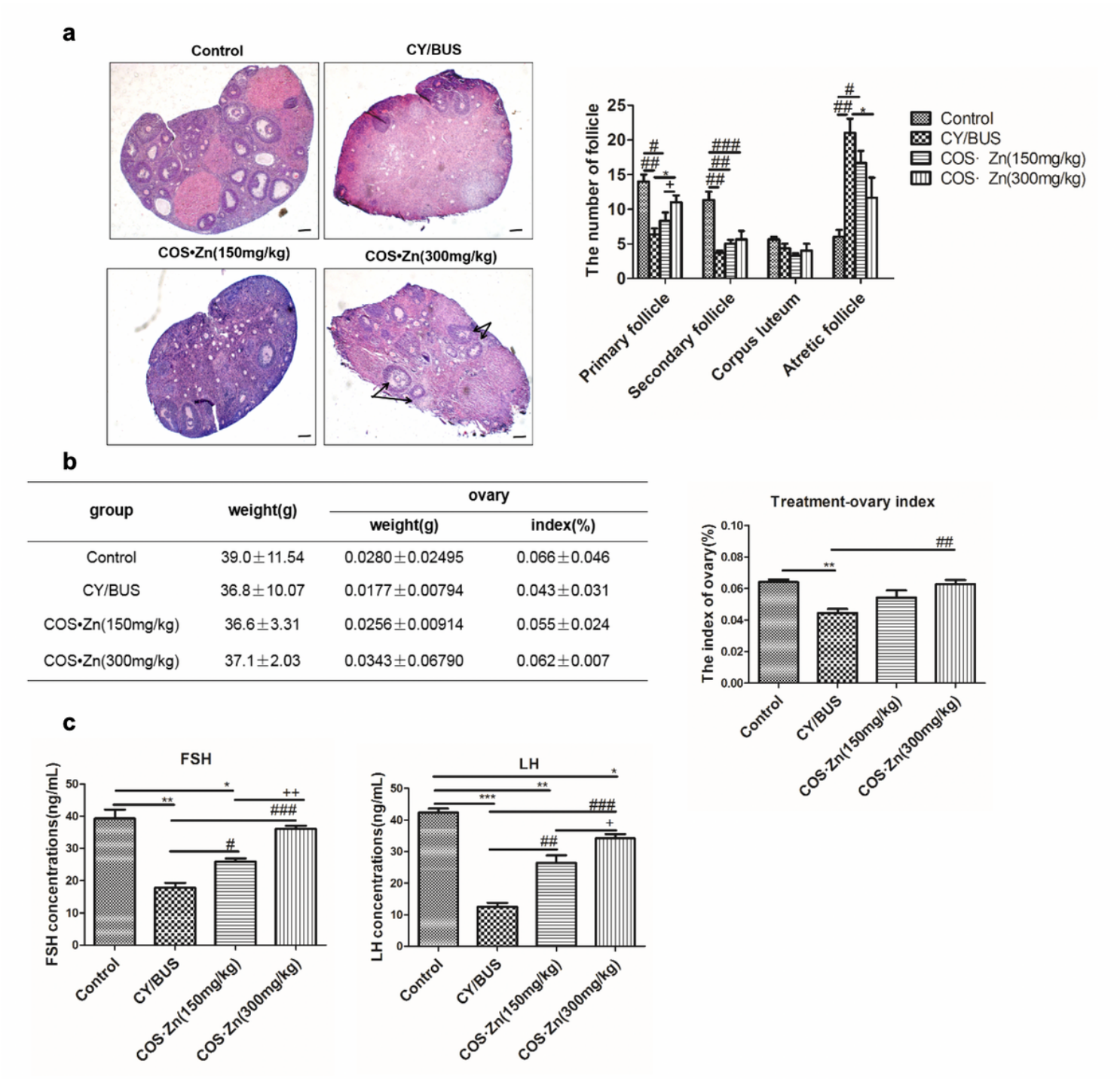

group	weight(g)	ovary	
		weight(g)	index(%)
Control	39.0±11.54	0.0280±0.02495	0.066±0.046
CY/BUS	36.8±10.07	0.0177±0.00794	0.043±0.031
COS•Zn(150mg/kg)	36.6±3.31	0.0256±0.00914	0.055±0.024
COS•Zn(300mg/kg)	37.1±2.03	0.0343±0.06790	0.062±0.007

Figure 2

COS•Znic effects the ovarian and follicular development in the treatment group. (a). Ovarian histology of COS·Zn-treated ovaries with various COS·Zn concentrations. Control group; CY/BUS group; 150mg/kg.d COS·Zn-treated mouse ovaries; 300mg/kg.d COS·Zn-treated mouse ovaries. The number of ovarian follicles and corpus luteum in different groups. (b) Effect of COS·Zn on ovarian index in treatment

groups. (c) Effect of COS·Zn on Follicle Stimulating Hormone(FSH) and Luteinizing Hormone(LH) levels in peripheral blood of treatment groups. *p<0.05, **p<0.01, ***p<0.001, compared with control group. #p<0.05, ##p<0.01, ###p<0.001, compared with CY/BUS group.

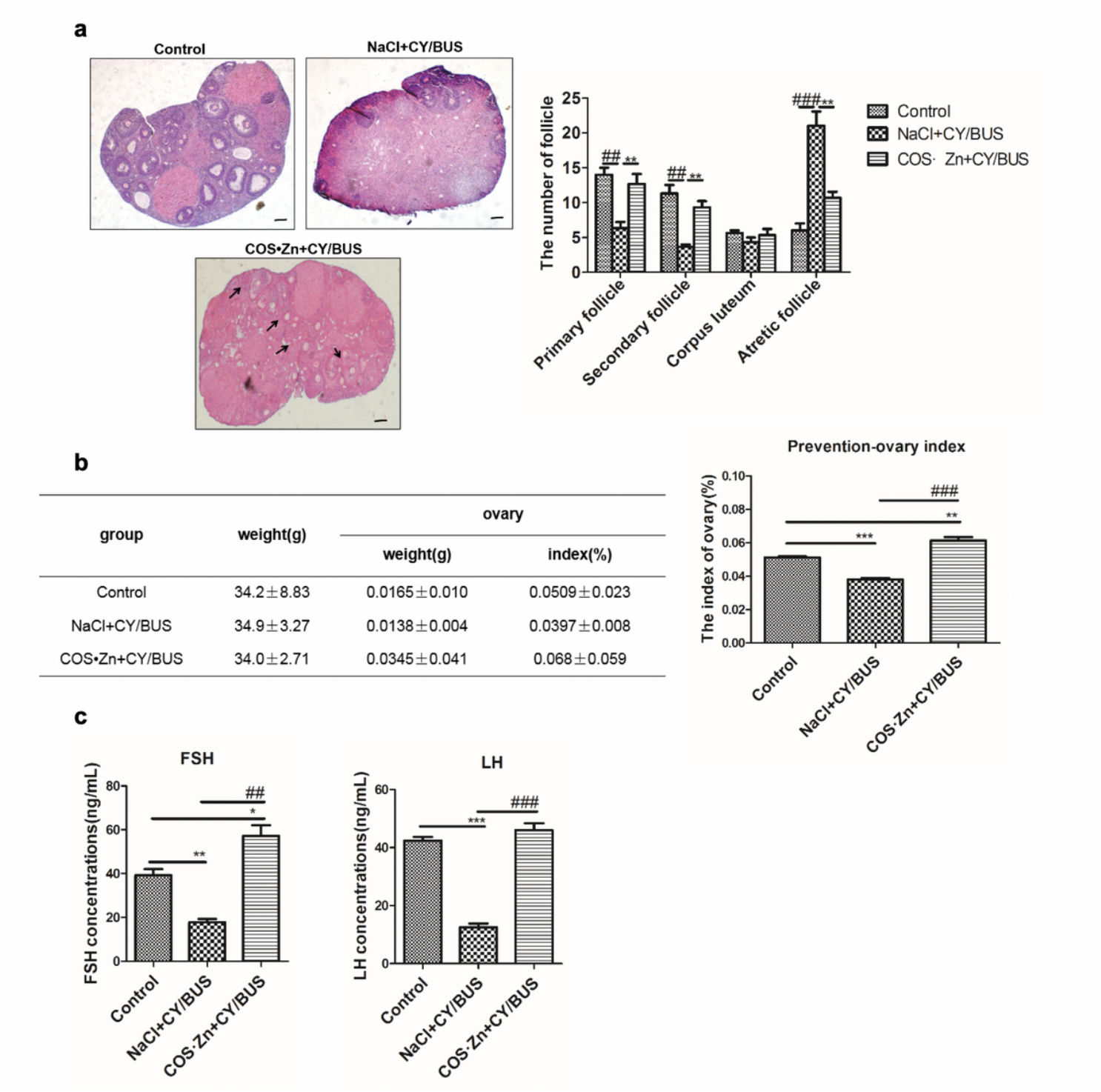

group	weight(g)	ovary	
		weight(g)	index(%)
Control	34.2±8.83	0.0165±0.010	0.0509±0.023
NaCl+CY/BUS	34.9±3.27	0.0138±0.004	0.0397±0.008
COS•Zn+CY/BUS	34.0±2.71	0.0345±0.041	0.068±0.059

Figure 3

COS•Znic effects the ovarian and follicular development in the prevention group. (a). Ovarian histology of NaCl and 300mg/kg.d.d COS·Zn-treated ovaries, respectively. Control group; CY/BUS-mouse ovaries. The number of ovarian follicles and corpus luteum in different groups. (b) Effect of COS·Zn on ovarian index

in prevention groups. (c) Effect of COS·Zn on Follicle Stimulating Hormone (FSH) and Luteinizing Hormone (LH) levels in peripheral blood of prevention groups. *p<0.05, **p<0.01, ***p<0.001, compared with control group. #p<0.05, ##p<0.01, ###p<0.001, compared with NaCl+CY/BUS group.

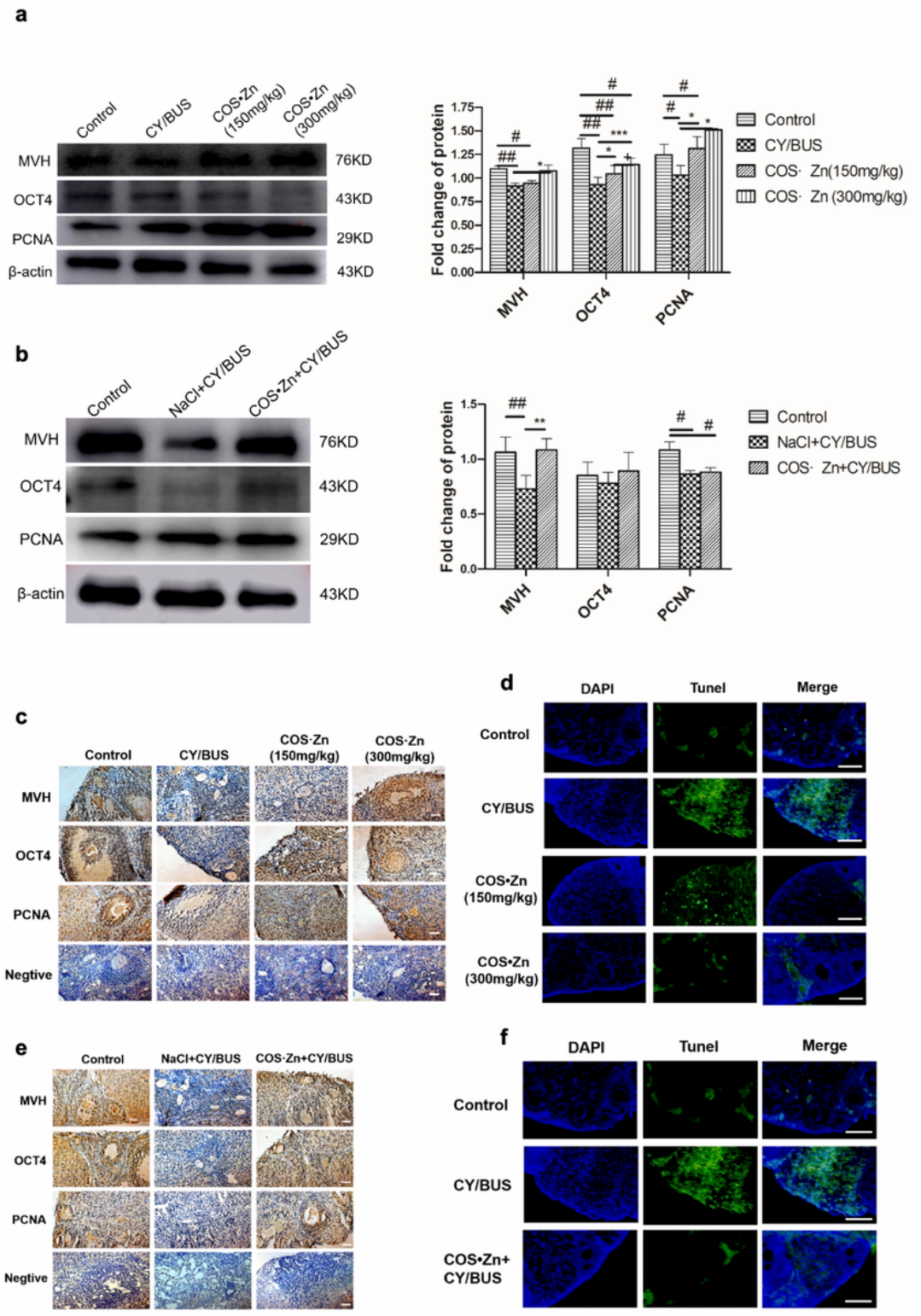

Figure 4

The expression of MVH/OCT4 genes during COS•Zn-treated ovaries in mice. (a,b) Western blotting showing the levels of MVH, OCT4 and PCNA during the treatment groups and the prevention groups. The

MVH, OCT4 and PCNA relative protein levels were assessed by densitometry analysis, calculated as relative to β-actin protein levels and expressed relative to levels in the different groups. Each value is the mean±SEM of determinations in five mice of each group. *: p < 0.05, **: p < 0.01, ***: p < 0.001 compared with control group. #p<0.05, ##p<0.01, compared with CY/BUS or NaCl+CY/BUS group. +p<0.05, compared with COS•Zn (150mg/kg·d) group. (c, e) Representative micrographs of ovarian sections from different mice stained immunohistochemically for MVH, OCT4 and PCNA. Scale bar: 100 μm. (d, f) apoptosis was detected by Tunnel. Scale bar: 100 μm.

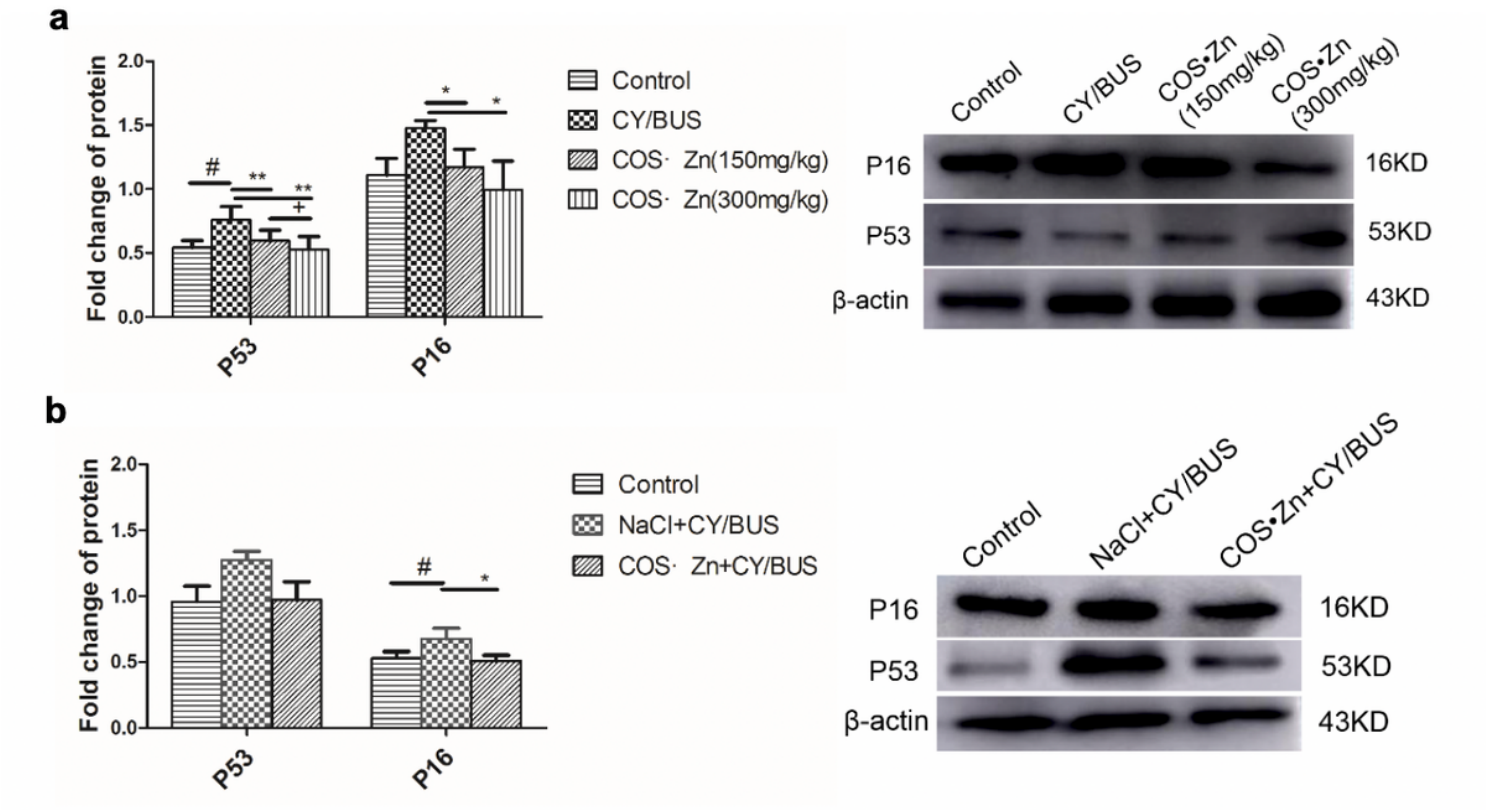

Figure 5

The expression of P53/P16 genes during COS•Zn-treated ovaries in mice by Western blotting during the treatment groups and prevention groups. (a,b) The P53/P16 relative protein levels were assessed by densitometry analysis, calculated as relative to β-actin protein levels and expressed relative to levels in the different groups. Each value is the mean±SEM of determinations in five mice of each group. *: p < 0.05, **: p < 0.01, ***: p < 0.001 compared with control group. #p<0.05, ##p<0.01, compared with CY/BUS or NaCl+CY/BUS group. +p<0.05, compared with COS•Zn(150mg/kg.d) group.

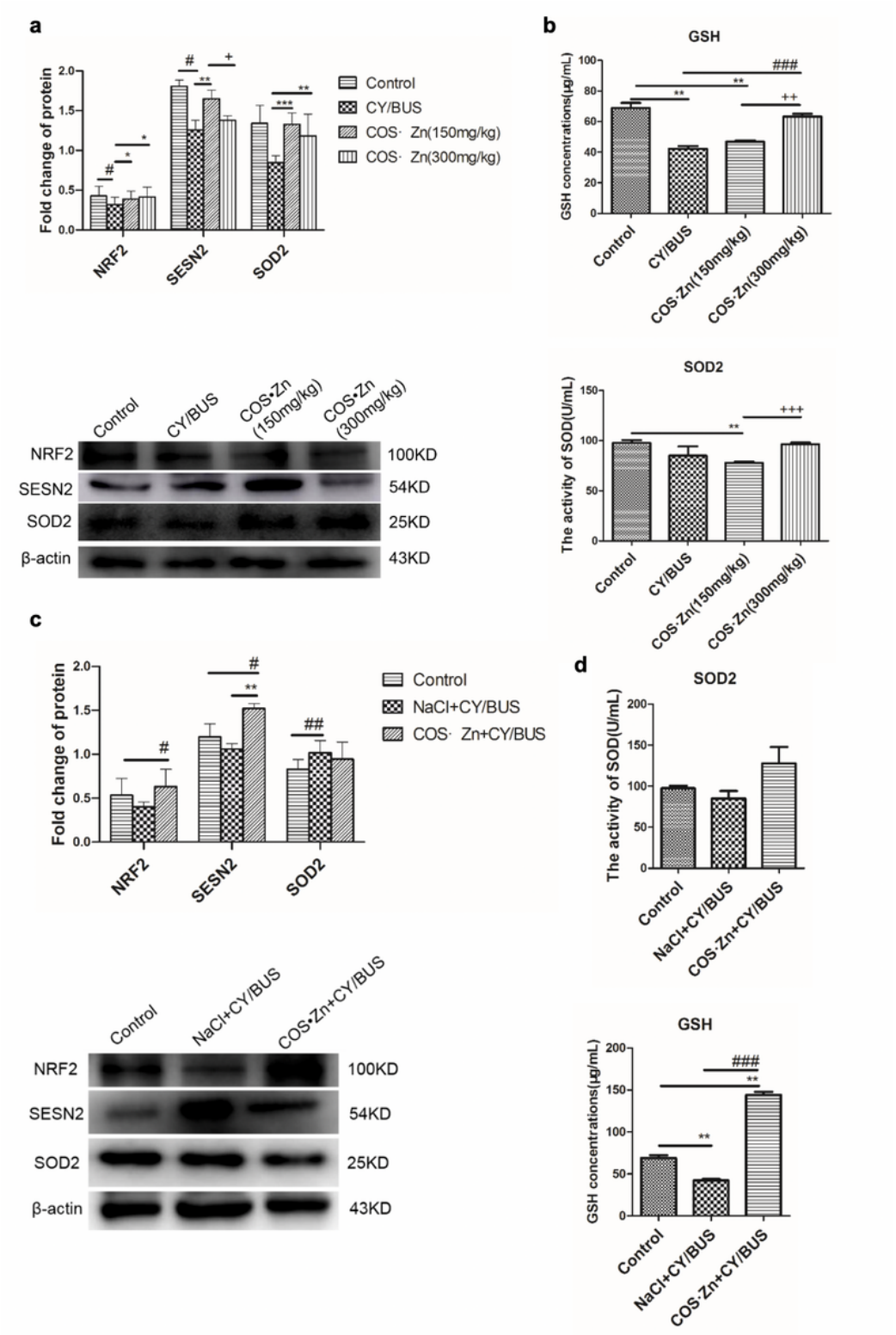

Figure 6

The expression of NRF2/SESN2/SOD2 genes during COS•Znic-treated ovaries in mice. (a) Western blotting showing the levels of NRF2, SESN2 and SOD2 during the treatemt groups. (b) Effect of COS·Zn on SOD2 and GSH levels in peripheral blood of the treatemt groups. (c)Western blotting showing the levels of NRF2, SESN2 and SOD2 during the prevention groups. (d) Effect of COS·Zn on Follicle SOD2 and GSH levels in peripheral blood of the prevention groups. (a,c):$p < 0.05$, **: $p < 0.01$, ***: $p < 0.001$

compared with CY/BUS or NaCl+CY/BUS group. #p<0.05, ##p<0.01, compared with control. +p<0.05, compared with COS•Zn(150mg/kg.d) group. (b,d)*: p < 0.05, **: p < 0.01, ***: p < 0.001 compared with control group. #p<0.05, ##p<0.01, compared with NaCl+CY/BUS group. +p<0.05, compared with COS•Zn(150mg/kg·d) group.